

Corrosion Inhibition Performance of 3,5-Diamino-1,2,4-triazole for Protection of Copper in Nitric Acid Solution

A. Zarrouk^{1,*}, B. Hammouti¹, S.S. Al-Deyab², R. Salghi³, H. Zarrok⁴, C. Jama⁵, F. Bentiss⁶

¹ Laboratory of Applied Chemistry and Environment (LCAE-URAC18), Faculté des Sciences, Université Mohammed Premier, B.P. 717, M-6000 Oujda, Morocco

² Petrochemical Research Chair, Chemistry Department, College of Science, King Saud University, P.O. Box 2455, Riyadh 11451, Saudi Arabia

³ Equipe de Génie de l'Environnement et de Biotechnologie, ENSA, Université Ibn Zohr, BP 1136, M-80000 Agadir, Morocco

⁴ Laboratoire des procédés de séparation, Faculté des Sciences, Kénitra, Morocco

⁵ Unité Matériaux et Transformations (UMET), Ingénierie des Systèmes Polymères, CNRS UMR 8207, ENSCL, BP 90108, F-59652 Villeneuve d'Ascq Cedex, France

⁶ Laboratoire de Chimie de Coordination et d'Analytique (LCCA), Faculté des Sciences, Université Chouaib Doukkali, B.P. 20, M-24000 El Jadida, Morocco

*E-mail: azarrouk@gmail.com

Received: 16 May 2012 / Accepted: 4 June 2012 / Published: 1 July 2012

The 3,5-diamino-1,2,4-triazole (DAT) is investigated as corrosion inhibitor for copper in 2 M HNO₃ medium by electrochemical techniques such as electrochemical impedance spectroscopy (EIS) and potentiodynamic polarization curves and weight loss measurements. Results show that DAT is a good corrosion inhibitor and its inhibition efficiency increases by increasing the inhibitor concentration. Changes in impedance parameters were indicative of adsorption of DAT on the copper surface, leading to the formation of protective films. Tafel polarization study revealed that DAT acts as a mixed type inhibitor. The inhibitor adsorption process in copper/DAT/nitric acid system was studied at different temperatures (303-343 K) by means of weight loss measurements. The adsorption of DAT on copper surface obeyed Langmuir's adsorption isotherm. The kinetic and thermodynamic parameters for copper corrosion and inhibitor adsorption, respectively, were determined and discussed.

Keywords: 1,2,4-Triazole; Copper; Nitric Acid; Corrosion inhibition; Adsorption

1. INTRODUCTION

Among all the metals, copper has been one of the most common metals used for industrial and domestic purposes due to its excellent electrical conductivity, good mechanical workability, low cost and other relatively noble properties. It is a material commonly used in heating and cooling systems,

and it is also used for electricity transportation due to its high conductance. A variety of environmental factors can easily cause corrosion of copper. Scale and corrosion products have a negative effect on heat transfer, and they cause a decrease in heating efficiency of the equipment. That is why periodic descaling and cleaning in hydrochloric acid and nitric acid pickling solutions are necessary. In order to reduce the corrosion of metals, several techniques have been applied. The use of chemical inhibitors is one of the most practical methods for the protection against corrosion in acidic media. Most of the excellent acid inhibitors are organic compounds containing nitrogen [1–13], oxygen [4, 13, 14–17], phosphorus [18] and sulphur [19–23]. Studies of the relation between adsorption and corrosion inhibition are of considerable importance.

Recently, we have investigated the inhibition effect of a 1,2,4-triazole derivative, namely 3-amino-1,2,4-triazole, on the corrosion of copper in 2 M nitric acid [2]. This compound acts as good inhibitor and the maximum of inhibition efficiency value is 82.2 % at 10^{-2} M. In continuation of our work on development of triazole derivatives as corrosion inhibitors in acidic media, we have studied the corrosion inhibiting behaviour of a novel 1,2,4-triazole derivative, namely 3,5-diamino-1,2,4-triazole (DAT), on copper in 2 M HNO₃ medium. Tafel polarization, electrochemical impedance spectroscopy (EIS) and weight loss measurements were used to evaluate the inhibition properties of DAT. The effect of concentration and temperature on the inhibition efficiency has been examined. The thermodynamic parameters for both activation and adsorption processes were calculated and discussed.

2. EXPERIMENTAL DETAILS

2.1. Materials

The investigated triazole, namely 3,5-diamino-1,2,4-triazole (DAT) is obtained from Sigma-Aldrich chemical co. and its chemical structure is presented in Fig. 1. The concentration range of the tested inhibitors employed in the inhibition study was 1×10^{-5} M to 1×10^{-2} M. The material used in this study is a copper with a chemical composition (in wt%) of 0.01 % Ni, 0.019 % Al, 0.004 % Mn, 0.116 % Si and 99.5 % Cu Prolabo Chemicals. Prior to all measurements, the copper samples were pre-treated by grinding with emery paper SiC (180, 600 and 2000); rinsed with distilled water, degreased in ethanol in an ultrasonic bath immersion for 5 min, washed again with bidistilled water and then dried at room temperature before use. The acid solutions (2 M HNO₃) were prepared by dilution of an analytical reagent grade 65% HNO₃ with doubly distilled water.

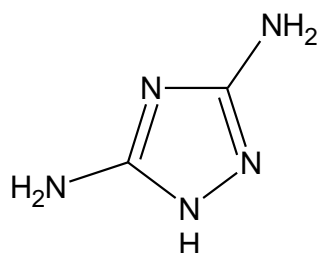


Figure 1. The molecular structure of DAT.

2.2. Electrochemical tests

2.2.1. Electrochemical cell

Electrochemical measurements were carried out in a conventional three-electrode cylindrical Pyrex glass cell. All electrochemical tests have been performed at 303 K in non-de-aerated solutions. The working electrode (WE) in the form of disc cut from copper has a geometric area of 0.28 cm^2 and is embedded in polytetrafluoroethylene (PTFE). A saturated calomel electrode (SCE) and a platinum electrode were used, as reference and auxiliary electrodes, respectively. A fine Luggin capillary was placed close to the working electrode to minimize ohmic resistance. The working electrode was immersed in test solution during 30 minutes until a steady state open circuit potential (E_{ocp}) was obtained.

2.2.2. Electrochemical impedance spectroscopy (EIS)

Electrochemical impedance spectroscopy experiments were conducted using Tacussel-Radiometer PGZ 3O1 and Voltamaster.4 Software was used to run the tests and to collect the experimental data. Ac impedance measurements were carried-out in the frequency range of 100 kHz to 10 mHz, with 10 points per decade, by applying 10 mV ac voltage peak-to-peak. Nyquist plots were made from these experiments. The best semicircle can be fit through the data points in the Nyquist plot using a non-linear least square fit so as to give the intersections with the x -axis.

2.2.3. Potentiodynamic polarization

Potentiodynamic polarization experiments were conducted using an electrochemical measurement system Tacussel Radiometer PGZ 301 controlled by a PC supported by Voltamaster.4 Software. The polarization curve was recorded by polarization from -150 to 150 mV versus E_{ocp} with a scan rate of 1 mV s^{-1} under air atmosphere.

2.3. Weight loss measurements

The gravimetric measurements were carried out at the definite time interval of 1 h at room temperature using an analytical balance (precision $\pm 0.1 \text{ mg}$). The copper specimens used have a rectangular form (length = 2 cm, width = 2 cm, thickness = 0.2 cm). Gravimetric experiments were carried out in a double glass cell equipped with a thermostated cooling condenser containing 50 ml of non-de-aerated test solution. After immersion period, the copper specimens were withdrawn, carefully rinsed with bidistilled water, ultrasonic cleaning in acetone, dried at room temperature and then weighted. Duplicate experiments were performed in each case and the mean value of the weight loss is calculated.

3. RESULTS AND DISCUSSION

3.1. Ac impedance study

The corrosion behaviour of copper, in acidic solution in the presence and absence of DAT compound, is investigated by the electrochemical impedance spectroscopy (EIS) at 303 K after 30 min of immersion. The polarization resistance (R_p) values are calculated from the difference in impedance at lower and higher frequencies, as suggested by Tsuru et al. [24]. To obtain the double layer capacitance (C_{dl}) the frequency at which the imaginary component of the impedance is maximal ($-Z_{max}$) is found as represented in the following equation where R_{ct} is the charge-transfer resistance:

$$C_{dl} = \frac{1}{2\pi f_{max} R_{ct}} \quad (1)$$

Nyquist plots recorded for copper electrode in 2M HNO₃ solution and containing various concentrations of DAT are shown in Fig. 2. As can be seen from this figure, the Nyquist plots do not yield perfect semicircles as expected from the EIS theory. The deviation from ideal semicircle was generally attributed to the frequency dispersion [25] as well as to the inhomogeneities of the surface and mass transport resistant [26]. In the evaluation of Nyquist plots, the difference in real impedance at lower and higher frequencies is generally considered as charge transfer resistance. The resistance between the metal and outer Helmholtz plane (OHP) must be equal to the charge-transfer resistance (R_{ct}) but in the present paper R_p was used instead of R_{ct} which has been discussed elsewhere [27,28].

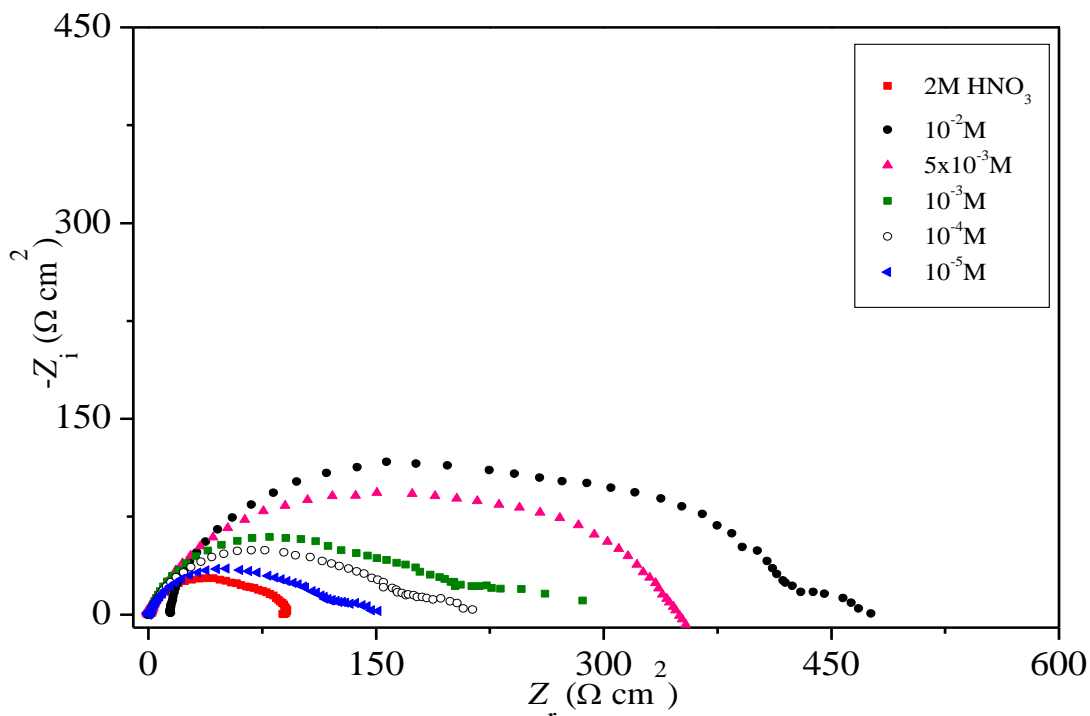


Figure 2. Impedance spectra obtained on the copper in 2 M HNO₃ in the presence of different concentration of DAT at 303 K.

Fig. 2 shows that the impedance response of copper has significantly changed by the addition of DAT to the corrosive solution and R_p values are bigger than that of uninhibited one and the impedance of inhibited substrate increases with increasing concentration of inhibitor in nitric acid. The impedance spectra of inhibited solutions consist of one depressed semicircle with a considerable deviation from an ideal semicircle. DAT molecules adsorb on the copper surface and modify the interface. The adsorption of inhibitor molecules on the metal surface decreases its electrical capacity because they displace the water molecules and other ions originally adsorbed on the metal surface [29]. This modification results in an increase of polarization resistance. The R_p values increased with DAT concentration may suggest the formation of a protective layer on the electrode surface. This layer makes a barrier for mass and charge transfers. The results show that R_p values increased with increase of inhibitor concentration. The electrochemical impedance parameters derived from the Nyquist plots and the inhibition efficiencies $E_Z(%)$ are shown in Table 1.

Table 1. Impedance parameters and inhibition efficiency values for copper in 2 M HNO₃ without and with different concentrations of DAT at 303 K.

C_{inh} (M)	R_p ($\Omega \text{ cm}^2$)	f_{max} (Hz)	C_{dl} ($\mu\text{F}/\text{cm}^2$)	E_Z (%)
Blank	91.4	15.82	110.1	—
1×10^{-5}	137.3	11.16	103.9	33.4
1×10^{-4}	193.9	7.94	103.4	52.9
1×10^{-3}	256.2	7.14	87.0	64.3
5×10^{-3}	351.2	5.62	80.7	74.0
1×10^{-2}	446.1	5.00	71.4	79.5

It is clear from Table 1 that by increasing the inhibitor concentration, the C_{dl} values tend to decrease and the inhibition efficiency increases. The decrease in C_{dl} values can be attributed to a decrease in local dielectric constant and/or an increase in the thickness of the electrical double layer, suggesting that DAT act by adsorption at the copper/solution interface [30]. On the other hand, the values of C_{dl} decreased with an increase in the inhibitor concentration. This behaviour was the result of an increase in the surface coverage by this inhibitor, which led to an increase in the inhibition efficiency. The thickness of the protective layer, δ_{org} , was related to C_{dl} by the following equation [31]:

$$\delta_{org} = \frac{\epsilon_0 \epsilon_r}{C_{dl}} \quad (3)$$

where ϵ_0 is the dielectric constant and ϵ_r is the relative dielectric constant. This decrease in the C_{dl} , which can result from a decrease in local dielectric constant and/or an increase in the thickness of the electrical double layer, suggested that DAT function by adsorption at the metal/solution interface.

Thus, the change in C_{dl} values was caused by the gradual replacement of water molecules by the adsorption of the organic molecules on the metal surface, decreasing the extent of metal dissolution [32]. The inhibition efficiency $E_Z(\%)$ is calculated, in the case of ac impedance method, by R_p using Eq. 2, where R_p^0 and R_p are the polarization resistance values without and with inhibitor [2], respectively :

$$E_Z(\%) = \frac{1/R_p^0 - 1/R_p}{1/R_p^0} \times 100 \quad (2)$$

From Table 1, is obvious that the increase in inhibitor concentration enhances R_p , and consequently improves the inhibition efficiency till reaching their maximum value at 10^{-2} M ($R_p = 446.1 \Omega \text{ cm}^2$, $E_Z(\%) = 79.5$).

3.2. Potentiodynamic polarization study

Polarization measurements have been carried out in order to gain knowledge concerning the kinetics of the anodic and cathodic reactions. The obtained Tafel polarization curves of copper in 2 M HNO₃ solution without and with different DAT concentrations are shown in Fig. 3. They show that the addition of the inhibitor hindered the acid attack of the copper electrode.

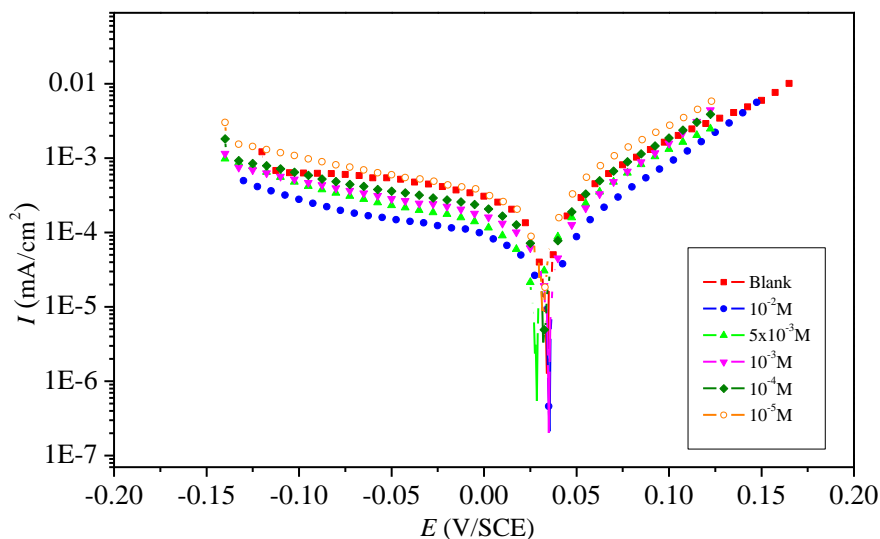


Figure 3. Potentiodynamic polarization curves of copper in 2 M HNO₃ for various concentrations of DAT at 303 K.

Electrochemical kinetic parameters (corrosion potential (E_{corr}), corrosion current density (I_{corr}) and cathodic Tafel slope (b_c)), determined from these experiments by extrapolation method, are

reported in Table 2. The inhibition efficiencies, $E_I(\%)$, are calculated from I_{corr} values using the following equation:

$$E_I(\%) = \frac{I_{corr}^o - I_{corr}}{I_{corr}^o} \times 100 \quad (4)$$

where I_{corr}^o and I_{corr} are the corrosion current densities for copper electrode in the uninhibited and inhibited solutions, respectively.

Table 2. Potentiodynamic polarization parameters for the corrosion of copper in 2 M HNO₃ without and with different concentrations of DAT.

C_{inh} (M)	E_{corr} (mV/SCE)	β_c (mV/dec)	I_{corr} ($\mu\text{A}/\text{cm}^2$)	E_I (%)
Blank	34	238	365.1	—
1×10^{-5}	32	229	265.2	27.4
1×10^{-4}	33	239	175.3	52.0
1×10^{-3}	35	237	126.9	65.2
5×10^{-3}	28	232	100.6	72.4
1×10^{-2}	35	265	071.9	80.3

As it is show in Fig. 3 and Table 2, cathodic current–potential curves give rise to parallel Tafel lines indicating that the hydrogen evolution reaction is under activation controlled. The cathodic current density decreases with the concentration of DAT however, a slight effect is observed on the anodic portions. This result indicates that DAT is adsorbed on the metal surface on the cathodic sites and hence inhibition occurs. These results demonstrate that the hydrogen reduction is inhibited and that the inhibition efficiency increases with inhibitor concentration to attain 80.3 % at 10⁻² M of DAT. The inhibition efficiency values, calculated from Tafel polarization method, show the same trend as those obtained from ac impedance study. We also remark that the inhibitor acts on the anodic portion and the anodic current density is reduced (Fig. 3). It seems also that the presence of the inhibitor change slightly the corrosion potential values in no definite direction. These results indicated that DAT acts as a mixed-type inhibitor.

3.3. Gravimetric measurements

3.3.1. Effect of concentration

The effect of addition of different concentrations of DAT on the corrosion of copper in 2 M HNO₃ solution was studied by weight loss measurements at 303 K for 1 h immersion period. For every

concentration, the mean value of the corrosion rate $C_R(\text{mg/cm}^2 \text{ h}^{-1})$ was determined and the inhibitor efficiency, $E_{WL}(\%)$, was calculated using Eqs. 5 and 6, respectively [34]:

$$C_R = \frac{W_b - W_a}{At} \quad (5)$$

$$E_{WL}(\%) = \left(1 - \frac{w_i}{w_0}\right) \times 100 \quad (6)$$

where W_b and W_a are the specimen weight before and after immersion in the tested solution, w_0 and w_i are the values of corrosion weight losses of copper in uninhibited and inhibited solutions, respectively, A the area of the copper specimen (cm^2) and t is the exposure time (h). Values of corrosion rates and inhibition efficiencies are given Table 3. The variations in the inhibition efficiency and corrosion rate with DAT concentration shown in Fig 4 suggest that DAT inhibits copper at all the concentration range used in the study. Maximum inhibition efficiency was reported at 10^{-2} M concentration of DAT. It is evident from the Table 3 that the corrosion rate (C_R) decreases and inhibition efficiency ($E_{WL} \%$) increases with increase in DAT concentration. The inhibition efficiency values, calculated from weight loss measurements, are in good agreement with those obtained from EIS and Tafel polarization techniques.

The corrosion resistance of copper in 2 M HNO_3 by another 1,2,4-triazole derivative, namely 3-amino-1,2,4-triazole (ATA) was previously described [2]. The variation in inhibitive efficiency mainly depends on the type and the nature of the substituent present in the inhibitor molecule. Indeed, the inhibition efficiency of ATA attains 82.2% at 10^{-2} M [2]. The substitution of hydrogen on the carbon (C5) of the triazole ring in ATA [2] by $-\text{NH}_2$ group in DAT (this work) arises an enhancement of the inhibition efficiency, from 82.2 % to 86.5% at 10^{-2} M, that may be due to the introduction of a strong electron releasing substituent on the triazole moiety, giving therefore a favourable electron density for preferential adsorption interactions. Hence it facilitates greater adsorption of DAT on copper surface than ATA, leading to higher inhibition efficiency of DAT than ATA.

Table 3. Corrosion parameters for copper in aqueous solution of 2 M HNO_3 in the absence and presence of different concentrations of DAT from weight loss measurements at 303K.

Inhibitor concentration (M)	C_R ($\text{mg/cm}^2 \text{ h}^{-1}$)	E_{WL} (%)
Blank	1.78	—
1×10^{-5}	1.19	33.3
5×10^{-5}	1.12	37.1
1×10^{-4}	0.85	52.5
5×10^{-4}	0.82	53.6
1×10^{-3}	0.54	69.7
5×10^{-3}	0.33	81.3
1×10^{-2}	0.24	86.5

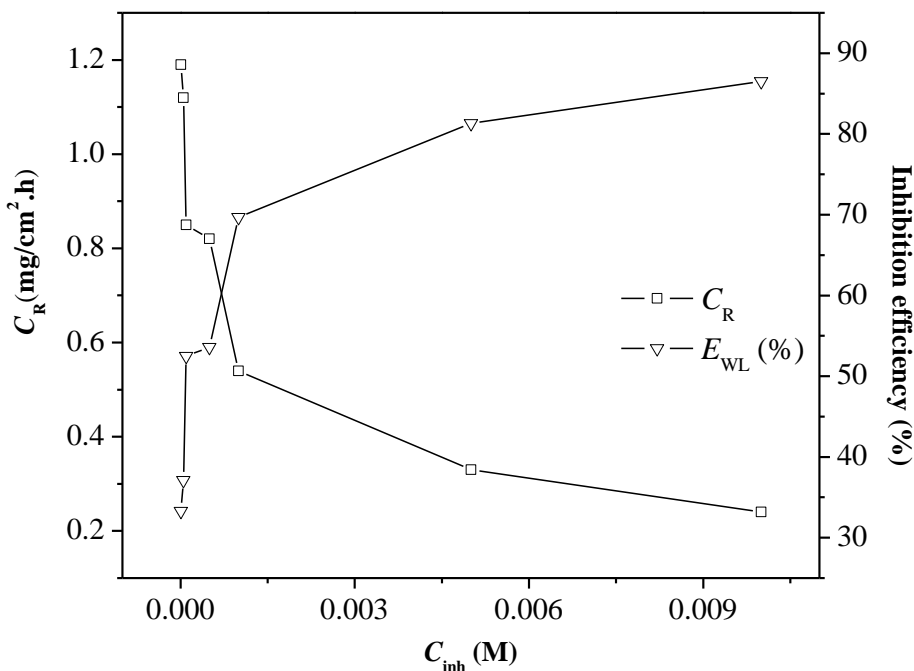


Figure 4. Variation of inhibition efficiency (E_{WL} %) and corrosion rate (C_R) in 2 M HNO_3 on copper surface without and with different concentrations of DAT.

3.3.2. Effect of temperature

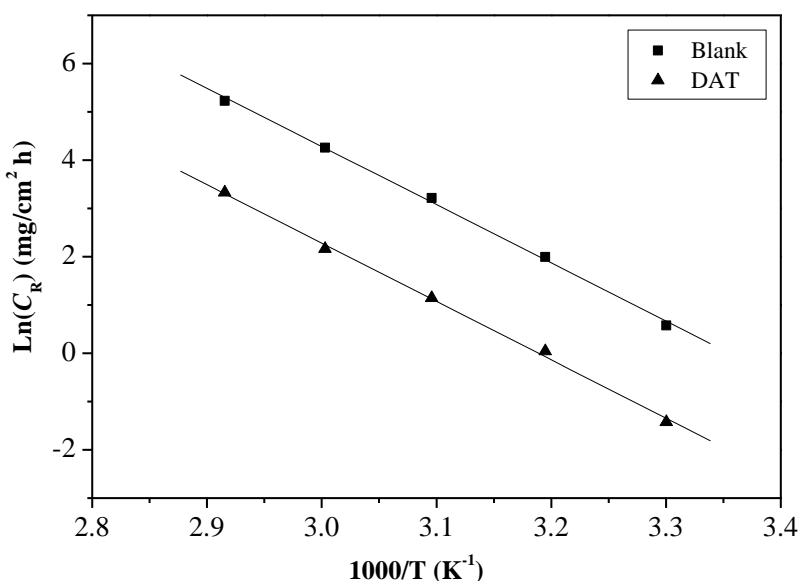


Figure 5. Arrhenius plots for copper corrosion rates (C_R) in 2 M HNO_3 in absence and in presence of 10^{-2} M of DAT.

The effect of temperature on the corrosion parameter of copper in 2 M HNO_3 was studied at 303 to 343K. The mechanism of inhibition can be deduced by comparing the activation energy in the presence and absence of the inhibitor. The Arrhenius plot and transition state plot were used to determine the activation energy (E_a), activation enthalpy (ΔH_a), and activation entropy (ΔS_a) for the

corrosion of copper in 2 M HNO₃ with and without 10⁻² M of DAT. The activation energy can be obtained by the Arrhenius equation and Arrhenius plot:

$$C_R = k \exp\left(-\frac{E_a}{RT}\right) \quad (7)$$

where E_a is the apparent activation corrosion energy, R is the universal gas constant, k is the Arrhenius pre-exponential factor and T is the absolute temperature. The linear regression plots between $\ln(C_R)$ and $1/T$ are presented in Fig.5.

The calculated activation energies, E_a , and pre-exponential factors, k , at different concentrations of the inhibitor are collected in Table 4. The change of the values of the apparent activation energies may be explained by the modification of the mechanism of the corrosion process in the presence of adsorbed inhibitor molecules [35]. Kinetic parameters such as enthalpy and entropy of corrosion process may be evaluated from the temperature effect. An alternative formulation of Arrhenius equation is [36]:

$$C_R = \frac{RT}{Nh} \exp\left(\frac{\Delta S_a}{R}\right) \exp\left(-\frac{\Delta H_a}{RT}\right) \quad (8)$$

where h is Plank's constant, N is Avogadro's number, ΔS_a is the entropy of activation and ΔH_a is the enthalpy of activation.

Fig. 6 shows a plot of $\ln(C_R/T)$ against $1/T$. A straight lines are obtained with a slope of $(-\Delta H_a/R)$ and an intercept of $(\ln R/Nh + \Delta S_a/R)$ from which the values of ΔH_a and ΔS_a are calculated and are listed in Table 4. The positive sign of the enthalpy (ΔH_a) reflects the endothermic nature of the copper dissolution process.

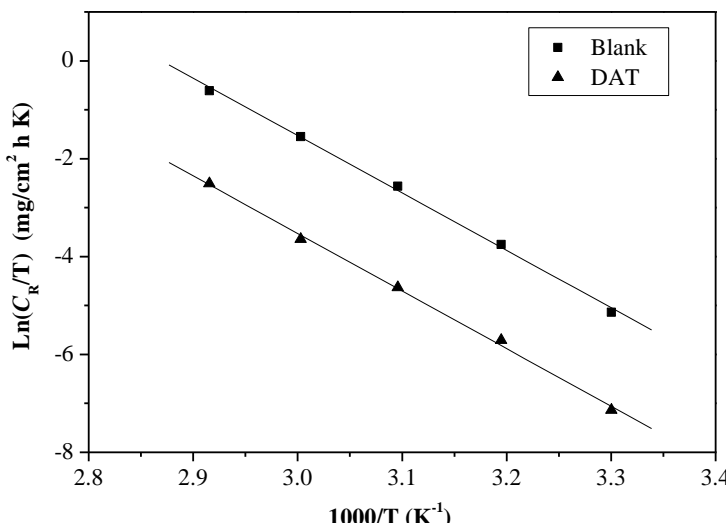


Figure 6. Transition-state plots for copper corrosion rates (C_R) in 2 M HNO₃ in absence and in presence of 10⁻² M of DAT.

The increase of E_a and ΔH_a accompanying the increase in the inhibitor concentration is explained by an increase of the energy barrier of corrosion reaction. The positive sign of the enthalpy (ΔH_a) reflects the endothermic nature of the copper dissolution process [36]. The higher activation energy in the inhibitor's presence further supports the proposed physisorption mechanism. Unchanged or lower values of E_a in inhibited systems compared to the blank to be indicative of chemisorption mechanism, while higher values of E_a suggest a physical adsorption mechanism. The positive values of entropy of activation (ΔS_a) are obtained in the presence of the inhibitor and in the absence. The entropy of activation (ΔS_a) decreased in the presence of DAT compared to free acid solution. As adsorption is an exothermic process and always accompanied by a decrease of entropy. Generally the adsorption of organic inhibitor molecules from the aqueous solution can be regarded as a quasi-substitution process between the organic compound in the aqueous phase and water molecules at the electrode surface [37]. In this situation, the adsorption of inhibitor is accompanied by desorption of water molecules from the copper surface. Thus, while the adsorption process for the inhibitor is believed to be exothermic and associated with a decrease in entropy of the solute, the opposite is true for the solvent.

Table 4. Corrosion kinetic parameters for copper in 2 M HNO₃ at 10⁻² M of DAT.

Medium	k (mg/cm ² h)	R ²	E _a (kJ/mol)	ΔH _a (kJ/mol)	ΔS _a (J/mol K)
Blank	3.66×10 ¹⁷	0.999	100.21	97.53	82.36
DAT	5.57×10 ¹⁶	0.999	100.53	97.85	66.69

3.3.3. Adsorption isotherm and thermodynamic activation parameters

It is widely acknowledged that adsorption isotherms provide useful insights onto the mechanism of corrosion inhibition as well as the interaction among the adsorbed molecules themselves and their interaction with the electrode surface [38]. Organic compounds adsorption can be described by two main types of interactions: physical adsorption (physisorption) and chemical adsorption (chemisorption). They are influenced by the nature of the charge of the metal, the chemical structure of the inhibitor and the type of electrolyte. Important information about the interaction between the inhibitor molecules and metal surface can be provided by the adsorption isotherm. The surface coverage (θ) suggests that a bond is formed between the metal atoms and the inhibitor molecules. The surface coverage is then a function of the electronic density on the functional atom(s) of the organic inhibitor; the molecules may be adsorbed on the metal/solution interface by the formation of either electrostatic or covalent bonds between the adsorbates and the metal surface atoms. Surface coverage data was useful in determining inhibitor adsorption characteristics. The fractional surface coverage (θ) can be easily determined from weight loss measurements by the ratio $E_{WL}(\%) / 100$, if one assumes that the values of $E_{WL}(\%)$ do no differ substantially from θ . Results of the present work were fitted to different isotherm type models to represent the adsorption behavior of DAT on copper surface [39] and the best fit was obtained with the Langmuir adsorption isotherm. The Langmuir adsorption isotherm

model has been used extensively in the literature for various metal, inhibitor and acid solution systems [40–42]. A plot of C_{inh}/θ versus C_{inh} (Fig. 7) gives a straight line with an average correlation coefficient of 0.999 and a slope of nearly unity (1.14) suggests that the adsorption of DAT molecules obeys Langmuir adsorption isotherm, which can be expressed by the following equation:

$$\frac{C_{\text{inh}}}{\theta} = \frac{1}{K_{\text{ads}}} + C_{\text{inh}} \quad (9)$$

where C_{inh} is the inhibitor concentration in the electrolyte and K_{ads} is the equilibrium constant of the adsorption process which is related to the standard Gibbs energy of adsorption, $\Delta G_{\text{ads}}^{\circ}$, according to:

$$K_{\text{ads}} = \frac{1}{55.55} \exp\left(\frac{-\Delta G_{\text{ads}}^{\circ}}{RT}\right) \quad (10)$$

where R is the universal gas constant, T the thermodynamic temperature and the value of 55.55 is the concentration of water in the solution in mol/L [43].

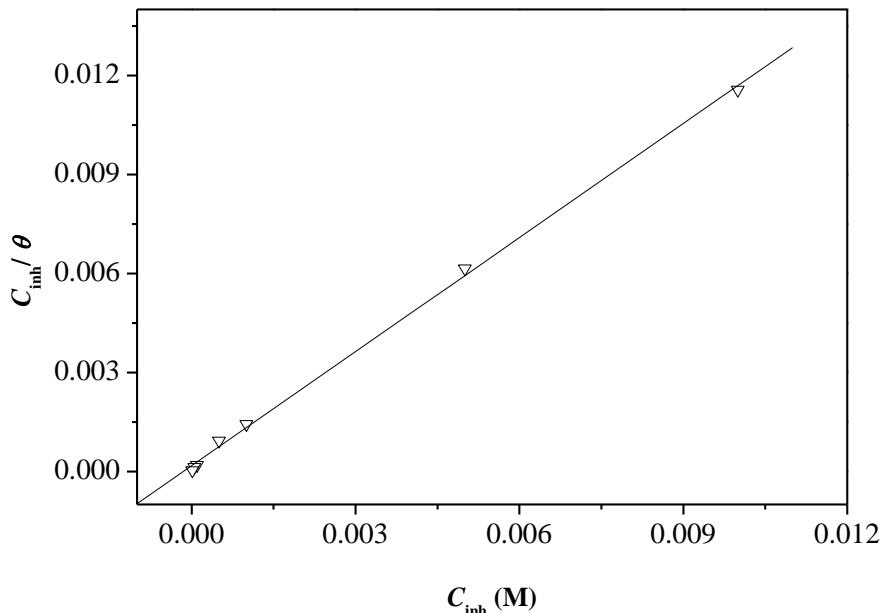
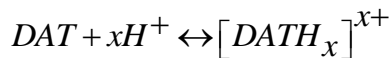


Figure 7. Langmuir adsorption isotherm for copper in 2 M HNO₃ containing different concentrations of DAT at 303 K.

The value K_{ads} calculated from the reciprocal of intercept of isotherm line as 5546.1 M⁻¹. The high value of the adsorption equilibrium constant reflects the high adsorption ability of this inhibitor on copper surface. From Eq. (8), the $\Delta G_{\text{ads}}^{\circ}$ was calculated as -31.83 kJ/mol. The negative value of

standard free energy of adsorption indicates spontaneous adsorption of triazole molecules on copper surface and also the strong interaction between inhibitor molecules and the metal surface [44, 45]. Generally, the standard free energy values of -20 kJ/mol or less negative are associated with an electrostatic interaction between charged molecules and charged metal surface (physical adsorption); those of -40 kJ/mol or more negative involves charge sharing or transfer from the inhibitor molecules to the metal surface to form a co-ordinate covalent bond (chemical adsorption) [46, 47]. The value of $\Delta G_{\text{ads}}^{\circ}$ in our measurement is -31.83 kJ/mol, it is suggested that the adsorption of DAT involves two types of interaction, chemisorption and physisorption [48]. Generally, Corrosion inhibition mechanism in acid medium is the adsorption of inhibitor onto the metal surface. As far as the inhibition process is concerned, it is generally assumed that adsorption of the inhibitor at the metal/solution interface is the first step in the action mechanism of the inhibitors in aggressive acid media. Four types of adsorption may take place during inhibition involving organic molecules at the metal/solution interface: (1) electrostatic attraction between charged molecules and the charged metal, (2) interaction of unshared electron pairs in the molecule with the metal, (3) interaction of π -electrons with the metal, and (4) a combination of the above [49]. Concerning inhibitors, the inhibition efficiency depends on several factors; such as the number of adsorption sites and their charge density, molecular size, heat of hydrogenation, mode of interaction with the metal surface, and the formation metallic complexes [50]. Physical adsorption requires presence of both electrically charged surface of the metal and charged species in the bulk of the solution; the presence of a metal having vacant low-energy electron orbital and of an inhibitor with molecules having relatively loosely bound electrons or heteroatom with lone pair electrons. However, the compound reported can be protonated in an acid medium. Thus they become cations, existing in equilibrium with the corresponding molecular form:



However, the protonated DAT could be attached to the copper surface by means of electrostatic interaction between NO_3^- and protonated DAT since the copper surface has positive charge in the 2 M HNO_3 medium. This could further be explained based on the assumption that in the presence of NO_3^- , the negatively charged NO_3^- would attach to positively charged surface and thereby protonated DAT being adsorbed to the metal surface.

4. CONCLUSIONS

The 3,5-diamino-1,2,4-triazole (DAT) shows good inhibition properties for the corrosion of copper in 2 M HNO_3 at 303 K, and the inhibition efficiency increases with increase in the inhibitor concentration. The inhibitor efficiencies determined by ac impedance, Tafel polarization and weight loss methods are in reasonable agreement. Based on the Tafel polarization results, DAT can be classified as mixed inhibitor. The inhibition efficiency $E(\%)$ of DAT is found to decrease proportionally with increasing temperature and its addition to 2 M HNO_3 leads to slight increase of

apparent activation energy (E_a) of corrosion process. The corrosion process is inhibited by the adsorption of DAT on copper surface and the adsorption of the inhibitor fits a Langmuir isotherm model at 303 K. Thermodynamic adsorption parameters show that DAT is adsorbed on copper surface by an exothermic, spontaneous process. Moreover, the calculated values of $\Delta G_{\text{ads}}^{\circ}$ reveal that the adsorption mechanism of DAT on copper surface in 2 M HNO₃ solution is mainly due to physisorption.

ACKNOWLEDGEMENTS

Prof. S.S. Al-Deyab and Prof B. Hammouti extend their appreciation to Deanship of Scientific Research at King Saud University for funding the work through the research group project 089.

References

1. Zarrouk, B. Hammouti, H. Zarrok, R. Salghi, A. Dafali, L. Bazzi, L. Bammou, S.S. Al-Deyab, *Der Pharm. Chem.* 4 (2012) 337–346.
2. Zarrouk, B. Hammouti, H. Zarrok, M. Bouachrine, K.F. Khaled, S.S. Al-Deyab, *Int. J. Electrochem. Sci.* 6 (2012) 89–105.
3. A. Zarrouk, B. Hammouti, A. Dafali, H. Zarrok, R. Touzani, M. Bouachrine, M. Zertoubi, *Res. Chem. Intermed.* (2011) DOI 10.1007/s11164-011-0444-2.
4. A. Zarrouk, B. Hammouti, H. Zarrok, S.S. Al-Deyab, M. Messali, *Int. J. Electrochem. Sci.* 6 (2011) 6261–6274.
5. A. Zarrouk, B. Hammouti, R. Touzani, S.S. Al-Deyab, M. Zertoubi, A. Dafali, S. Elkadiri, *Int. J. Electrochem. Sci.* 6 (2011) 4939–4952.
6. A. Zarrouk, B. Hammouti, A. Dafali, M. Bouachrine, H. Zarrok, S. Boukhris, S.S. Al-Deyab, *J. Saudi Chem. Soc.* (2011) doi:10.1016/j.jscs.2011.09.011.
7. A. Zarrouk, B. Hammouti, A. Dafali, H. Zarrok, *Der Pharm. Chem.* 3 (2011) 266–274
8. A. Zarrouk, T. Chelfi, A. Dafali, B. Hammouti, S.S. Al-Deyab, I. Warad, N. Benchat, *Int. J. Electrochem. Sci.* 5 (2010) 696–705.
9. M.A. Ameer, E. Khamis, G. Al-Senani, *J. Appl. Electrochem.* 32 (2002) 149–156.
10. F. Bentiss, M. Traisnel, L. Gengembre, M. Lagrenée, *Appl. Surf. Sci.* 161 (2000) 194–202.
11. E.E. Ebenso, *Mater. Chem. Phys.* 79 (2003) 58–70.
12. S.S. Abd El-Rehim, S.A.M. Refaey, F. Taha, M.B. Saleh, R.A. Ahmed, *J. Appl. Electrochem.* 31 (2001) 429–435.
13. K. F. Khaled, Mohammed A. Amin, *Corros. Sci.* 51 (2009) 2098–2106.
14. F. Bentiss, M. Traisnel, N. Chaibi, B. Mernari, H. Vezin, M. Lagrenée, *Corros. Sci.* 44 (2002) 2271–2285.
15. F. Bentiss, M. Lagrenée, M. Traisnel, B. Mernari, H. El. Attari, *J. Appl. Electrochem.* 29 (1999) 1073–1078.
16. M. Hosseini, S.F.L. Mertens, M. Ghorbani, M.R. Arshadi, *Mater. Chem. Phys.* 78 (2003) 800–808.
17. M.A. Migahed, H.M. Mohamed, A.M. Al-Sabagh, *Mater. Chem. Phys.* 80 (2003) 169–175.
18. E. Khamis, E.S.H. EI-Ashry, A.K. Ibrahim, *Br. Corros. J.* 35 (2000) 150–154.
19. H.L. Wang, H.B. Fan, J.S. Zheng, *Mater. Chem. Phys.* 77 (2003) 655–661.
20. M.A. Quraishi, H.K. Sharma, *Mater. Chem. Phys.* 78 (2002) 18–21.
21. A. Popova, E. Sokolova, S. Raicheva, M. Christov, *Corros. Sci.* 45 (2003) 33–58.
22. L. Larabi, O. Benali, Y. Harek, *Port. Electrochim. Acta* 24 (2006) 337–346.
23. A. Fiala, A. Chibani, A. Darchen, A. Boulkamh, K. Djebbar, *Appl. Surf. Sci.* 253 (2007) 9347–9356.

24. T. Tsuru, S. Haruyama, B. Gijutsu, *J. Jpn. Soc. Corros. Eng.* 27 (1978) 573–581.
25. M. El Achouri, S. Kertit, H.M. Gouttaya, B. Nciri, Y. Bensouda, L. Perez, M.R. Infante, K. Elkacemi, *Prog. Org. Coat.* 43 (2001) 267–273.
26. S. Ramesh, S. Rajeswari, *Electrochim. Acta* 49 (2004) 811–820.
27. M. Erbil, *Chim. Acta Turcica*. 1 (1988) 59–70.
28. T. Tuken, B. Yazıcı, M. Erbil, Proceedings of Ninth European Symposium on Corrosion Inhibitors (9 SEIC), N.S., Sez. V, Suppl. 11, Ann. Univ. Ferrara, 2000, p. 115.
29. M. Lebrini, M. Lagrenée, H. Vezin, L. Gengembre, F. Bentiss, *Corros. Sci.* 47 (2005) 485–505.
30. M. Elayyachy, A. El Idrissi, B. Hammouti, *Corros. Sci.* 48 (2006) 2470–2479.
31. S. Martinez, M. Metikos-Hukovic, *J. Appl. Electrochem.* 33 (2003) 1137–1142.
32. F. Bentiss, M. Lagrenée, B. Mehdi, B. Mernari, M. Traisnel, H. Vezin, *Corrosion* 58 (2002) 399–407.
33. S.S. Abd El-Rehim, M.A.M. Ibrahim, K.F. Khaled, *J. Appl. Electrochem.* 29 (1999) 593–599.
34. S.R. Lodha, *Pharmaceutical Reviews* 6 (2008) 1.
35. O. Riggs, I. R. Hurd, M. Ray, *Corrosion*. 23 (1967) 252–258.
36. J.O.M. Bochris, A.K.N. Reddy, *Modern Electrochem.* Plenum Press, New York, 2 (1977) 1267.
37. M. Sahin, S. Bilgic, H. Yilmaz, *Appl. Surf. Sci.* 195 (2002) 1–7.
38. A.N. Wiercinska, G. Dalmata, *Electrochim. Acta* 51 (2006) 6179–6185.
39. E.E. Oguzie, C. Unaegbu, C.N. Ogukwe, B.N. Okolue, A.I. Onuchukwu, *Mater. Chem. Phys.* 84 (2004) 363–368.
40. G. Mu, X. Li, G. Liu, *Corros. Sci.* 47 (2005) 1932–1952.
41. R. Fuchs-Godec, *Coll. Surf. A Physicochem. Eng. Asp.* 280 (2006) 130–139.
42. F. Bentiss, M. Lebrini, M. Lagrenée, *Corros. Sci.* 47 (2005) 2915–2931.
43. O. Olivares, N.V. Likhanova, B. Gomez, J. Navarrete, M.E. Llanos-Serrano, E. Arce, J.M. Hallen, *Appl. Surf. Sci.* 252 (2006) 2894–2909.
44. G. Avci, *Mater. Chem. Phys.* 112 (2008) 234–238.
45. E. Bayol, A.A. Gurten, M. Dursun, K. Kayakırılmaz, *Acta Phys. Chim. Sin.* 24 (2008) 2236–2242.
46. O.K. Abiola, N.C. Oforka, *Mater. Chem. Phys.* 83 (2004) 315–322.
47. M. Ozcan, R. Solmaz, G. Kardas, I. Dehri, *Colloid. Surf. A* 325 (2008) 57–63.
48. S. Zhang, Z. Tao, W. Li, B. Hou, *Appl. Surf. Sci.* 255 (2009) 6757–6763.
49. D. Schweinsberg, G. George, A. Nanayakkara, D. Steinert, *Corros. Sci.* 28 (1988) 33–42.
50. A. Fouda, M. Moussa, F.I. Taha, A.I. Elneanaa, *Corros. Sci.* 26 (1986) 719–726.